Retrodictions of late Paleogene Mantle Flow

Hans-Peter Bunge

Ludwig-Maximilians University (LMU) München

L. Colli, S. Ghelichkhan, J. Oeser, M. Mohr, B. Schuberth, L. Vynnytska,
A. Horbach, A. Friedrich, R. Pail

(LRZ, SAMPLE-SPP, TOPO-AFRICA)

Collège de France
December 1st, 2016

OUTLINE

- Introduction (forward models, dynamic topography)
- Theory (equations, twin experiments on convergence, boundary conditions)
- Simple Geodynamic Earth Models (model initialisation and uniqueness)
- Retrodictions (sensitivity to model parameters and tomographic input model)
- Conclusions (retrodictions are an powerful tool to learn about past Earth dynamics)

Global Mantle Convection Models

- Achievements
  - **many of them**
  - high resolution
  - comp. efficient
  - scenario simulations
- Frontiers
  - forward vs. inverse
  - link to observation
  - explicit histories

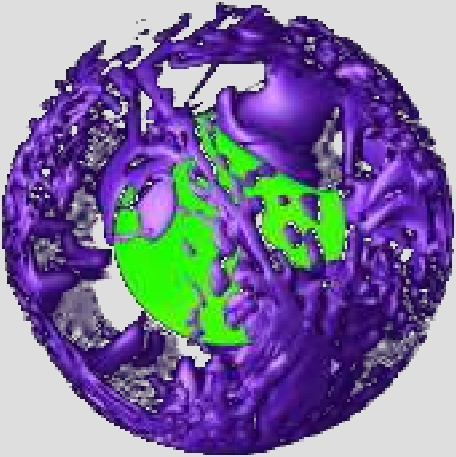

(Zurich group)

Global Mantle Convection Models

- Achievements
  - **many of them**
  - high resolution
  - comp. efficient
  - scenario simulations
- Frontiers
  - forward vs. inverse
  - link to observation
  - explicit histories

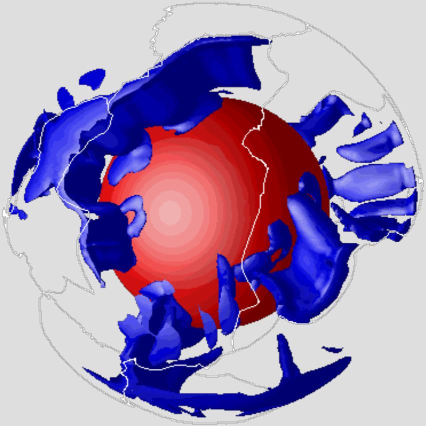

(Boulder group)

Global Mantle Convection Models

- Achievements
  - **many of them**
  - high resolution
  - comp. efficient
  - scenario simulations
- Frontiers
  - forward vs. inverse
  - link to observation
  - explicit histories

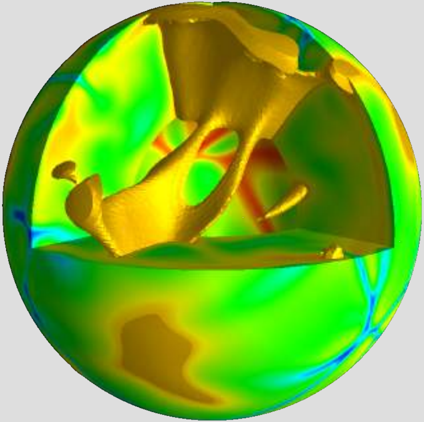

(Munich group)

Global Mantle Convection Models

- Achievements
  - many of them
  - **high resolution (10^9 grid points)**
  - comp. efficient
  - scenario simulations
- Frontiers
  - forward vs. inverse
  - link to observation
  - explicit histories

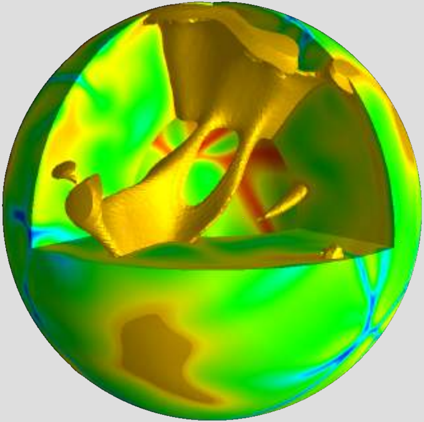

(Munich group)

Global Mantle Convection Models

- Achievements
  - many of them
  - high resolution
  - **comp. efficient**
  - scenario simulations
- Frontiers
  - forward vs. inverse
  - link to observation
  - explicit histories

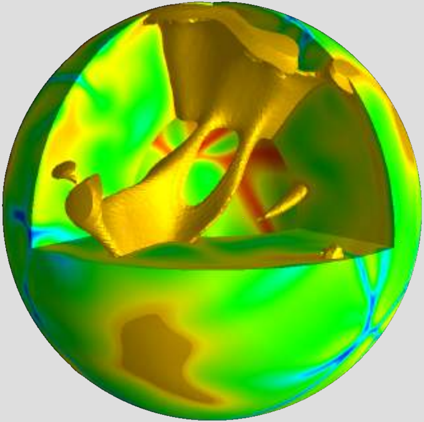

(Munich group)

Global Mantle Convection Models

- Achievements
  - many of them
  - high resolution
  - comp. efficient
  - **scenario simulations**
- Frontiers
  - forward vs. inverse
  - link to observation
  - explicit histories

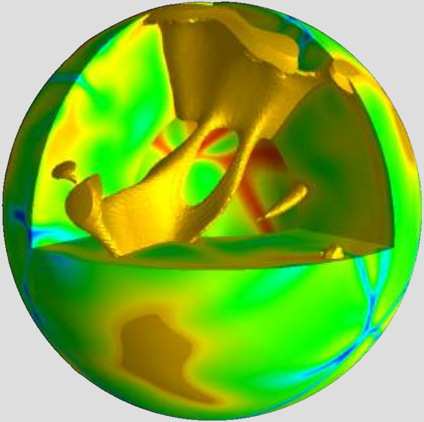

(Munich group)

Global Mantle Convection Models

- Achievements
  - many of them
  - high resolution
  - comp. efficient
  - scenario simulations
- Frontiers
  - **forward vs. inverse**
  - link to observation
  - explicit histories

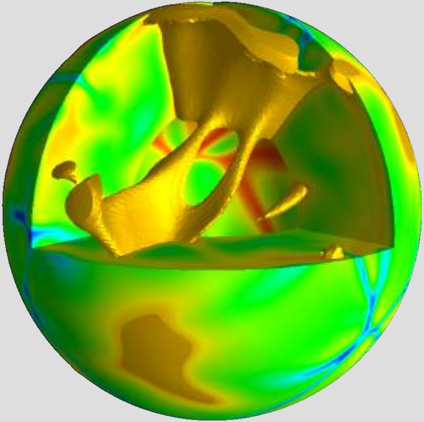

(Munich group)

Global Mantle Convection Models

- Achievements
  - many of them
  - high resolution
  - comp. efficient
  - scenario simulations
- Frontiers
  - forward vs. inverse
  - **link to observation**
  - explicit histories

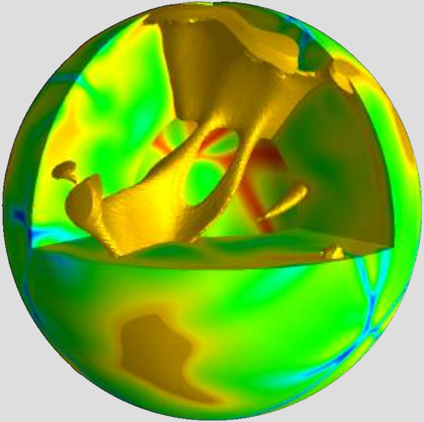

(Munich group)

Global Mantle Convection Models

- Achievements
  - many of them
  - high resolution
  - comp. efficient
  - scenario simulations
- Frontiers
  - forward vs. inverse
  - link to observation
  - **explicit histories**

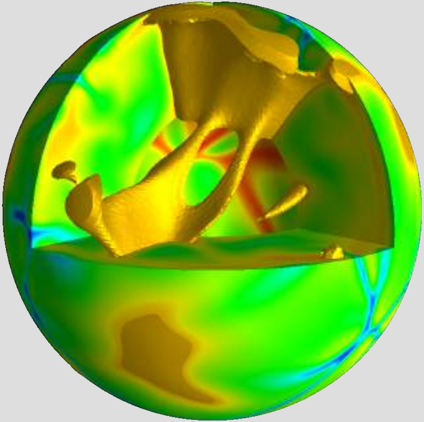

(Munich group)

Record of (late Mesozoic/Cenozoic) vertical motion:

paleo shorelines

5 Myr:

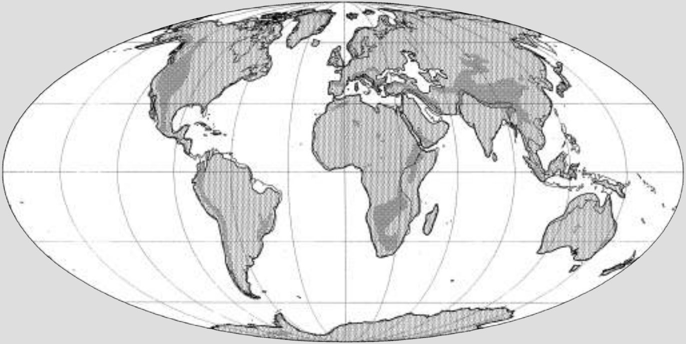

(modified from Paleogeographic atlas)

Record of (late Mesozoic/Cenozoic) vertical motion:

paleo shorelines

10 Myr:

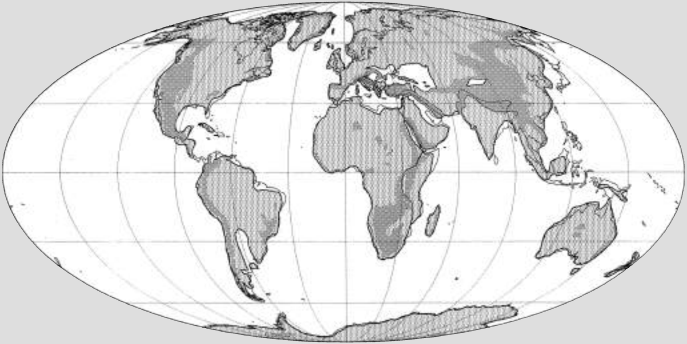

(modified from Paleogeographic atlas)

Record of (late Mesozoic/Cenozoic) vertical motion:

paleo shorelines

20 Myr:

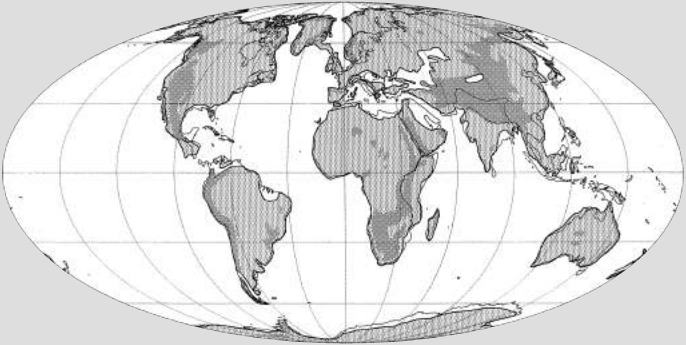

(modified from Paleogeographic atlas)

Record of (late Mesozoic/Cenozoic) vertical motion:

paleo shorelines

30 Myr:

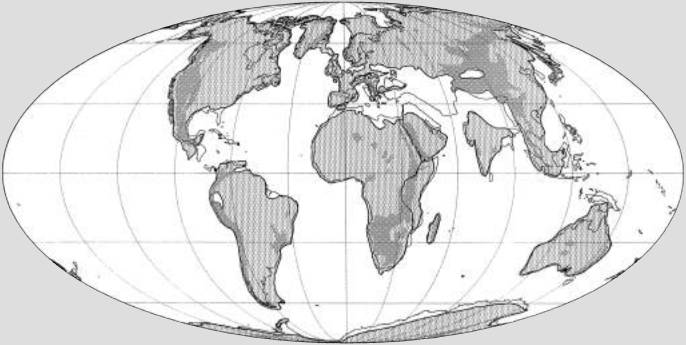

(modified from Paleogeographic atlas)

Record of (late Mesozoic/Cenozoic) vertical motion:

paleo shorelines

45 Myr:

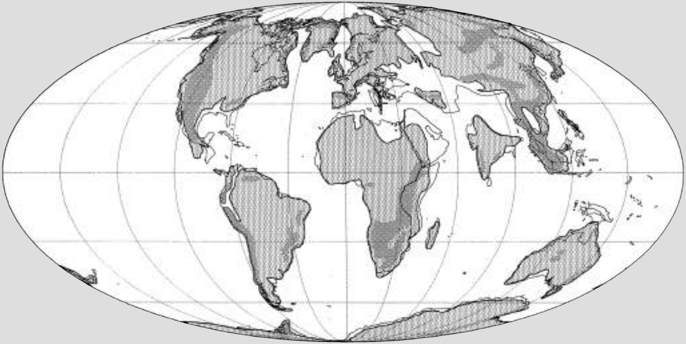

(modified from Paleogeographic atlas)

Record of (late Mesozoic/Cenozoic) vertical motion:

paleo shorelines

60 Myr:

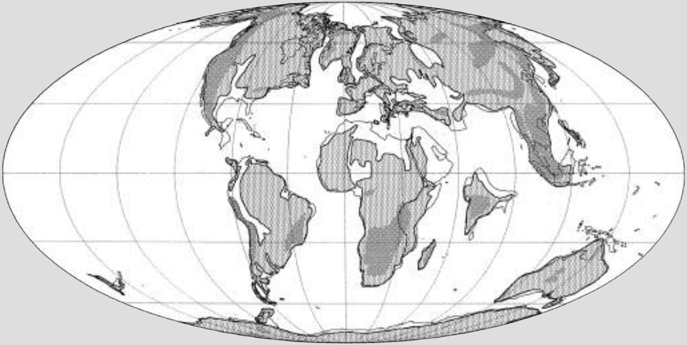

(modified from Paleogeographic atlas)

Record of (late Mesozoic/Cenozoic) vertical motion:

paleo shorelines

70 Myr:

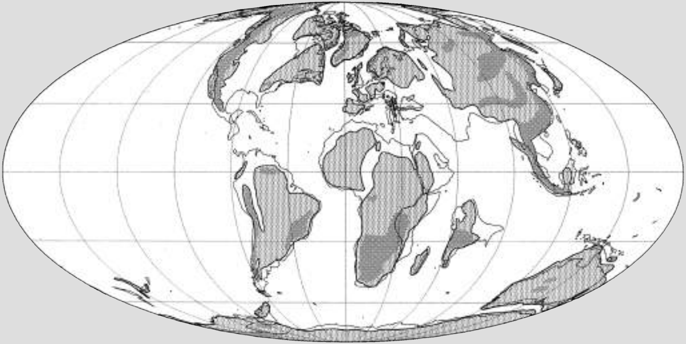

(modified from Paleogeographic atlas)

Record of (late Mesozoic/Cenozoic) vertical motion:

paleo shorelines

80 Myr:

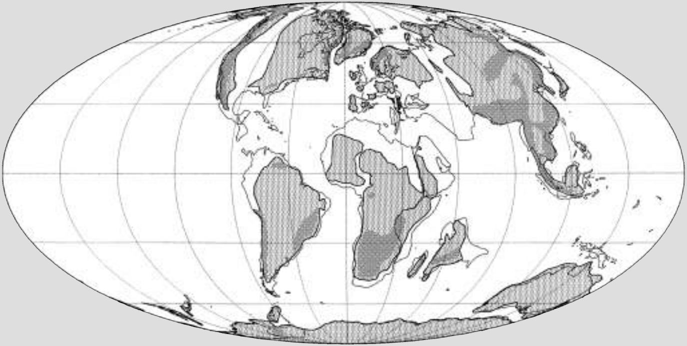

(modified from Paleogeographic atlas)

Record of (late Mesozoic/Cenozoic) vertical motion:

paleo shorelines

90 Myr:

(modified from Paleogeographic atlas)

Africas Elevation History

- **Topo Africa**: French sister program of the German **DFG SAMPLE SPP** to study the topographic evolution of Africa.

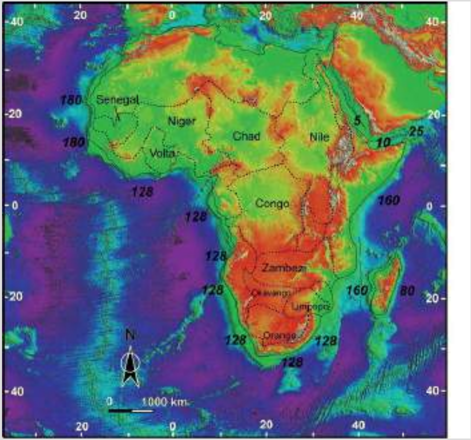

Burke & Gunnell. (2008)

Gravity and Dynamic Topography

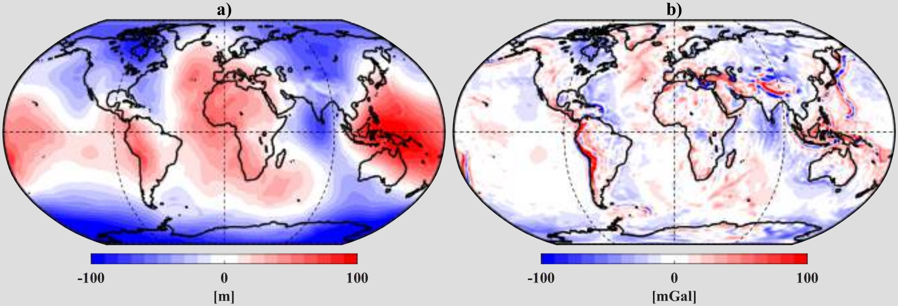

Colli et al. (2016)

Response Kernels of Dynamic Earth Models

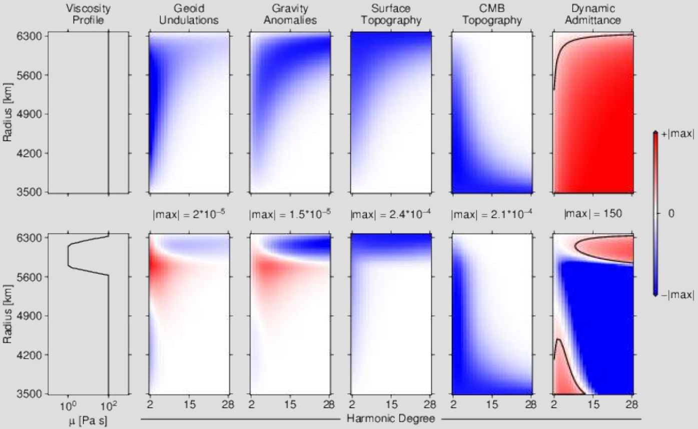

Colli et al. (2016)

Admittance vs. Wavelength

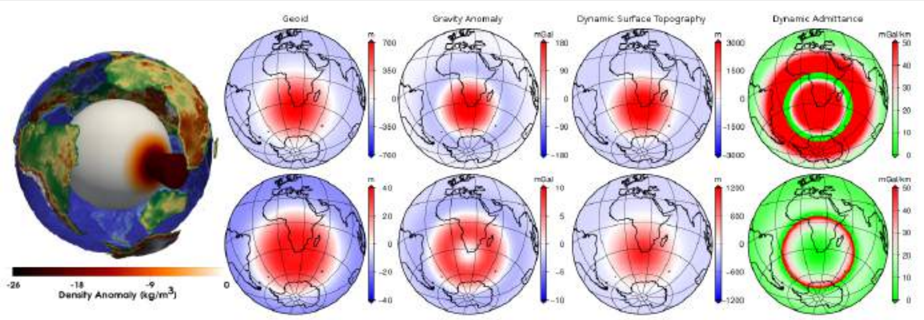

Colli et al. (2016)

The **inverse approach** to geodynamic flow modeling

The initial condition problem

Initial state estimates from which one may start a model

a) Run convection models for a long time (with surface velocities given by known plate motion histories), i.e. longer than one mantle overturn, $\approx$ 150 Ma.

b) run convection backward in time (e.g., Moucha et al., Steinberger et al.)

$\Rightarrow$ c) pose fluid dynamic inverse problem based on history matching

The Adjoint equations of mantle convection

Mathematical procedures (chain rule, partial integration, adjoint operators) lead to the adjoint equations:

$$\partial_t \Psi + v \cdot \nabla \Psi + k \nabla^2 \Psi + \alpha \rho_0 g \cdot \phi = \partial_T \hat{\chi}(T)$$
$$\nabla \cdot \eta \Big(\nabla \phi + (\nabla \phi)^T \Big) + \Psi \nabla T = 0$$
$$\nabla \cdot \phi = 0$$

The scalar field Ψ is the so called *adjoint temperature*. It has to satisfy the above equations and provides sensitivity information about the initial state.

The Adjoint equations of mantle convection

Mathematical procedures (chain rule, partial integration, adjoint operators) lead to the adjoint equations:

$$
\begin{aligned}
&\partial_t \Psi + v \cdot \nabla \Psi + k \nabla^2 \Psi + \alpha \rho_0 g \cdot \phi = \partial_T \hat{\chi}(T) \\
&\nabla \cdot \eta \left(\nabla \phi + (\nabla \phi)^T \right) + \Psi \nabla T = 0 \\
&\nabla \cdot \phi = 0
\end{aligned}
$$

The scalar field Ψ is the so called *adjoint temperature*. It has to satisfy the above equations and provides sensitivity information about the initial state.

The Adjoint equations of mantle convection

We solve the *adjoint* equations in global mantle flow models

- terminal condition on temperature
- adjoint diffusion operator stable vs. time-reversal
- iterative procedure: computationally expensive, but is beginning to become feasible in 3D

$\Rightarrow$ **optimise for suitable flow histories (backwards in time)**

The (variational) adjoint approach to data assimilation

By iteratively adjusting the initial condition, one corrects the model trajectory over the whole time window, providing an *optimal* fit to the observational (here terminal condition) constraints.

Dashed line corresponds to initial (unconstrained) guess of the model trajectory.

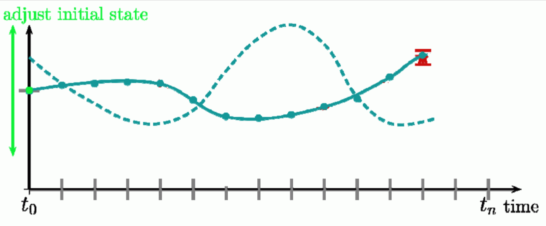

(From **Fournier et al. 2012** with an application to dynamo models. Similiar approaches are used in meteorology, oceanography, glacier dynamics, hydrology.)

The compressible adjoint equations of mantle convection

Mathematical procedures (chain rule, partial integration, adjoint operators) lead to the *compressible* adjoint equations:

$$\partial_t \Psi + v \cdot \nabla \Psi - (\gamma - 1)\Psi \nabla \cdot v + k \nabla^2 \Psi + \alpha \rho_0 g \cdot \phi = \partial_T \hat{\chi}(T)$$
$$\nabla \cdot \eta \left(\nabla \phi + (\nabla \phi)^T \right) + \Psi \nabla T = 0$$
$$\nabla \cdot \phi = 0$$

The scalar field Ψ is the so called adjoint temperature. It has to satisfy the above equations and provides sensitivity information about the initial state.
(from **Ghelichkhan & Bunge, 2016**)

The compressible adjoint equations of mantle convection

Mathematical procedures (chain rule, partial integration, adjoint operators) lead to the *compressible* adjoint equations:

$$\partial_t \Psi + v \cdot \nabla \Psi - (\gamma - 1)\Psi \nabla \cdot v + k \nabla^2 \Psi + \alpha \rho_0 g \cdot \phi = \partial_T \hat{\chi}(T)$$
$$\nabla \cdot \eta \left(\nabla \phi + (\nabla \phi)^T \right) + \Psi \nabla T = 0$$
$$\nabla \cdot \phi = 0$$

The scalar field Ψ is the so called adjoint temperature. It has to satisfy the above equations and provides sensitivity information about the initial state.
(from **Ghelichkhan & Bunge, 2016**)

inverse mantle convection models

Twin Experiments (convergence)

Twin Experiments

Evolve Reference Twin from *initial* to *final* state.

Time period corresponding to 50 Myrs ($\approx 1/2$ overturn).

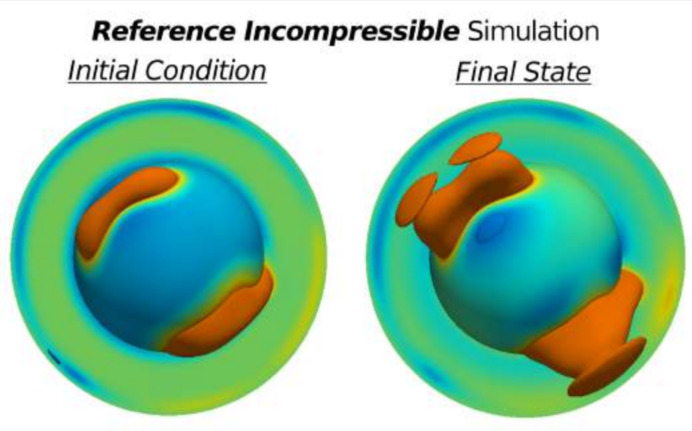

Initial and final state for reference twin (red=hot, blue=cold).
(from **Ghelichkhan & Bunge, 2016**)

Twin Experiments

Iterate the adjoint many times from *initial* to *final* state.

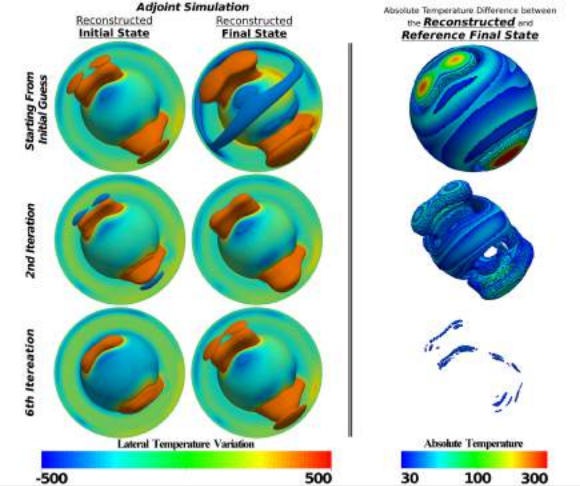

Initial and final state reconstructions for increasing (top to bottom: 0,2,6) iterations (red=hot, blue=cold). Note that the initial state error is nearly eliminated through the inversion after 6 iterations. (from **Ghelichkhan & Bunge, 2016**)

Twin Experiments

Convergence per iteration for *initial* and *final* state compared to reference twin.

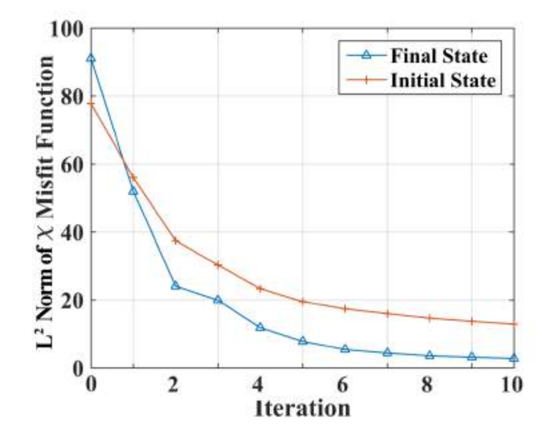

Initial and final state residual. (from **Ghelichkhan & Bunge, 2016**)

regularisation of the inversion through knowledge of the surface velocity field

Twin Experiments: surface velocity

Evolve reference convection model (Twin) from *initial* to *final* state.

Pick a time period corresponding to 50 Myrs
($\approx 1/2$ overturn).

See, if one recovers the intial state.

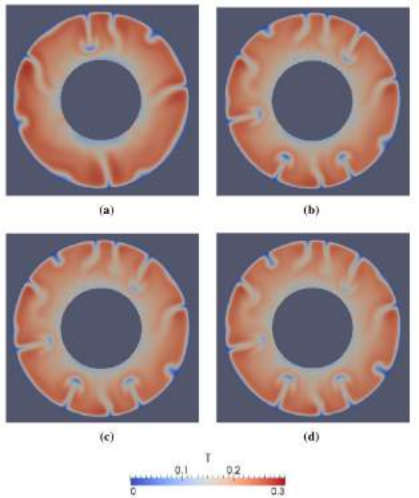

(a-d) temperatures (red=hot, blue=cold) at initial (a), intermediate (b,c) and final (d) state, (from **Vynnytska & Bunge, 2014**)

Twin Experiments: surface velocity

First guess for *initial* condition.

Take a simple 1-D profile as the *first guess* for the unknown temperature of the initial state.

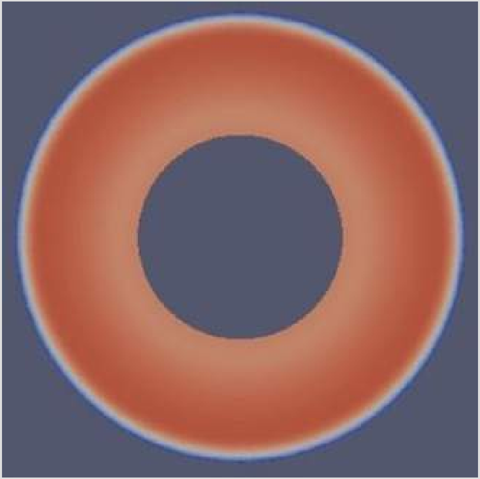

First guess model temperature initial condition (from **Vynnytska & Bunge, 2014**)

Twin Experiments: surface velocity

First guess for *initial* condition.

Take a simple 1-D profile as the *first guess* for the unknown temperature of the initial state.

This unrealistic *first guess* state is equivalent to assuming there is *no convection*.

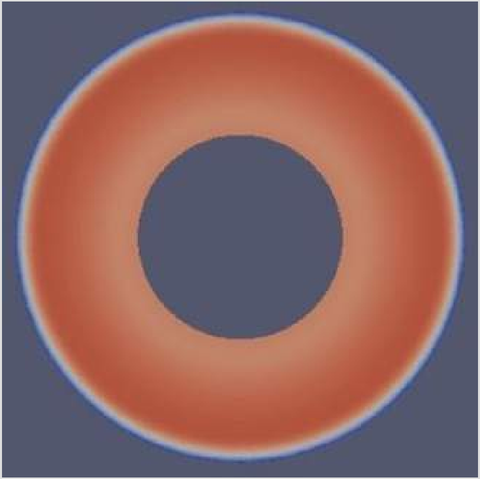

First guess model temperature initial condition (from **Vynnytska & Bunge, 2014**)

Twin Experiments

Recovered initial state temperature after **20** forward and adjoint iterations.

Left with assimilated history of model surface velocities.

Right with unconstrained (free slip) model surface.

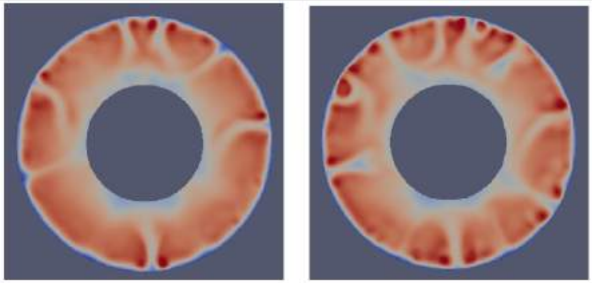

first guess model temperature initial condition (from **Vynnytska & Bunge, 2014**)

The inversion is *unsuccessful* with unconstrained (free slip) model surface.

Twin Experiments

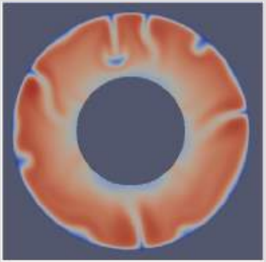

True model temperature initial condition (from **Vynnytska & Bunge, 2014**)

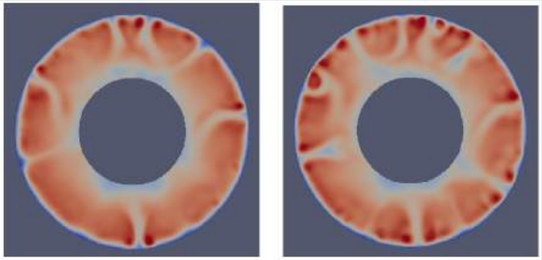

Best guess model temperature initial condition with assimilated (left) and unconstrained surface velocities (right)
(from **Vynnytska & Bunge, 2014**)

The inversion is **unsuccessful** for model (right most) with unconstrained surface velocities. It succeeds, when the **history of surface velocities** is known.

Twin Experiments

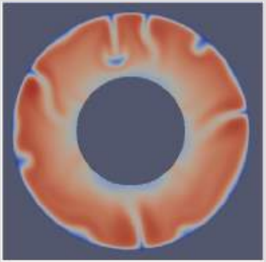

True model temperature initial condition (from **Vynnytska & Bunge, 2014**)

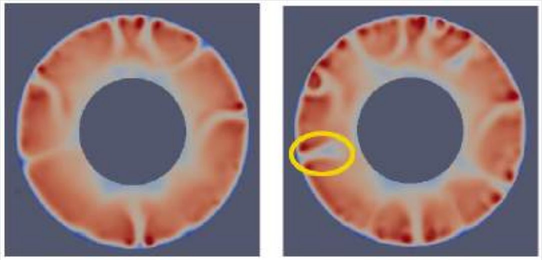

Best guess model temperature initial condition with assimilated (left) and unconstrained surface velocities (right)
(from **Vynnytska & Bunge, 2014**)

The inversion is **unsuccessful** for model (right most) with unconstrained surface velocities. It succeeds, when the **history of surface velocities** is known.

Twin Experiments

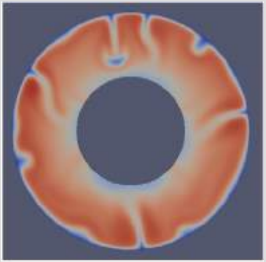

True model temperature initial condition (from **Vynnytska & Bunge, 2014**)

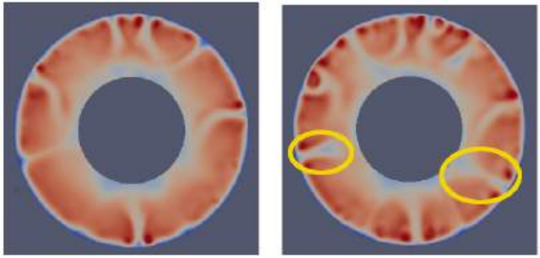

Best guess model temperature initial condition with assimilated (left) and unconstrained surface velocities (right)
(from **Vynnytska & Bunge, 2014**)

The inversion is **unsuccessful** for model (right most) with unconstrained surface velocities. It succeeds, when the **history of surface velocities** is known.

Twin Experiments

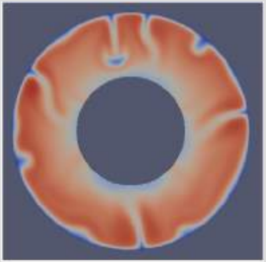

True model temperature initial condition (from **Vynnytska & Bunge, 2014**)

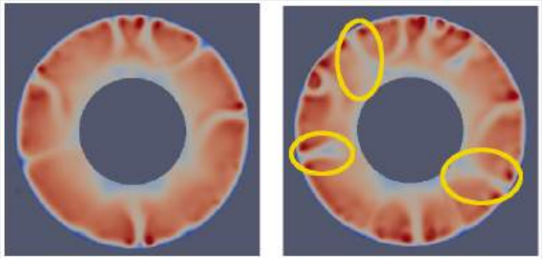

Best guess model temperature initial condition with assimilated (left) and unconstrained surface velocities (right)
(from **Vynnytska & Bunge, 2014**)

The inversion is **unsuccessful** for model (right most) with unconstrained surface velocities. It succeeds, when the **history of surface velocities** is known.

Twin Experiments

Initial State
RMS error as a function of adjoint iteration

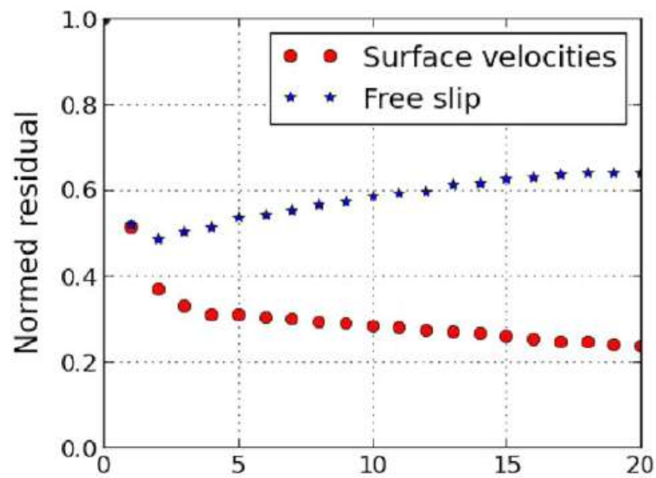

(from **Vynnytska & Bunge, 2014**)

Twin Experiments

Initial State
RMS error as a function of adjoint iteration

(note divergence for model with *free-slip* surface)

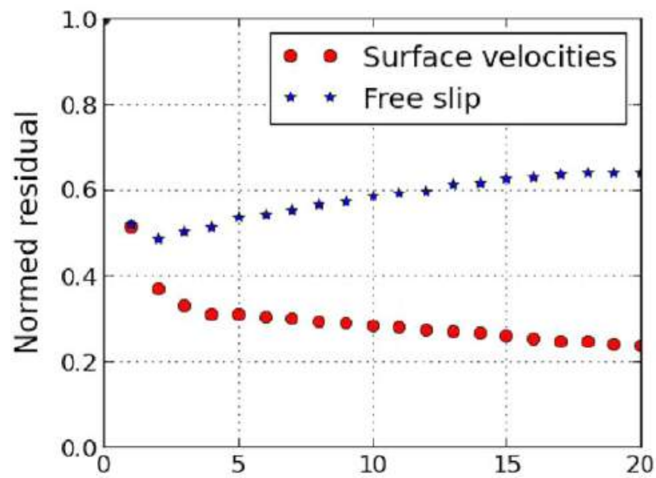

(from **Vynnytska & Bunge, 2014**)

Twin Experiments

Initial State
RMS error as a function of adjoint iteration

(note divergence for model with *free-slip* surface)
(we understand this result as a consequence of Serrin's *uniqueness* theorem)

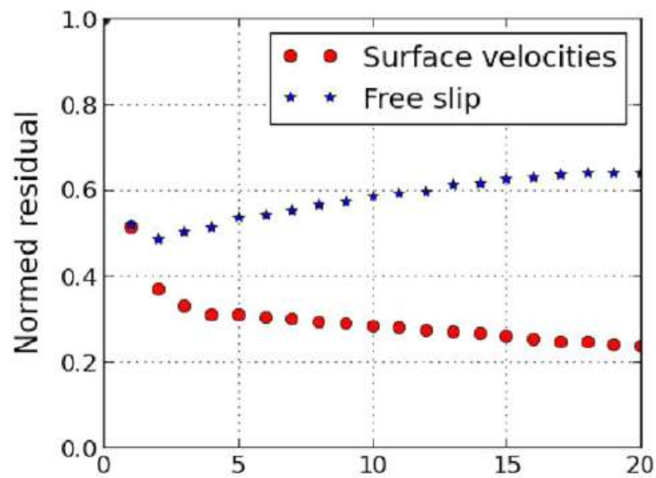

(from **Vynnytska & Bunge, 2014**)

Twin Experiments

Final State
RMS error as a function of adjoint iteration.

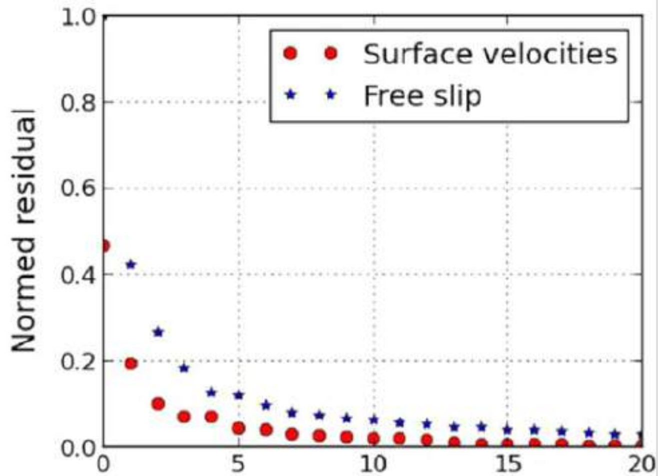

(from **Vynnytska & Bunge, 2014**)

Twin Experiments

Final State
RMS error as a function of adjoint iteration.

(note there is convergence, i.e. the cost function is reduced, for either model)

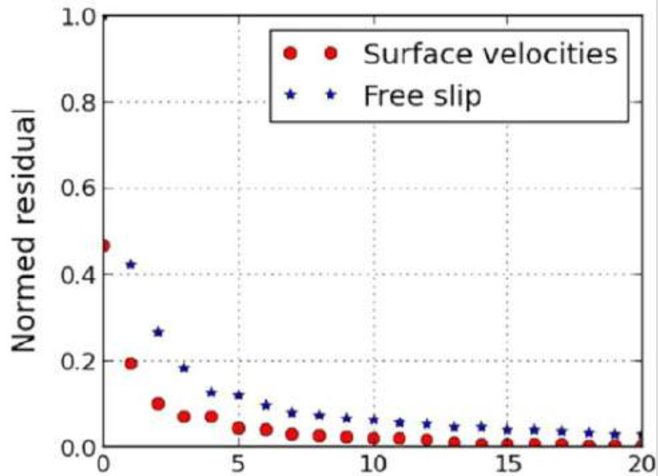

(from **Vynnytska & Bunge, 2014**)

Record of past (late Mesozoic/Cenozoic) plate motion:

horizontal motion of Earth's surface is reconstructed for past $\approx$ 200 million years

provides boundary condition for velocity

one effectively exploits Serrin's theorem

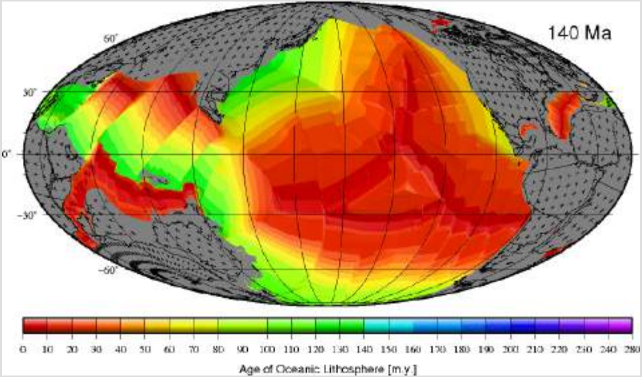

Record of past (late Mesozoic/Cenozoic) plate motion:

horizontal motion of Earth's surface is reconstructed for past $\approx$ 200 million years

provides boundary condition for velocity

one effectively exploits Serrin's theorem

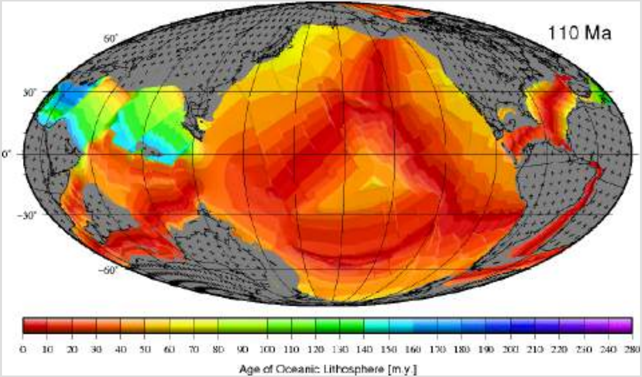

Record of past (late Mesozoic/Cenozoic) plate motion:

horizontal motion of Earth's surface is reconstructed for past $\approx$ 200 million years

provides boundary condition for velocity

one effectively exploits Serrin's theorem

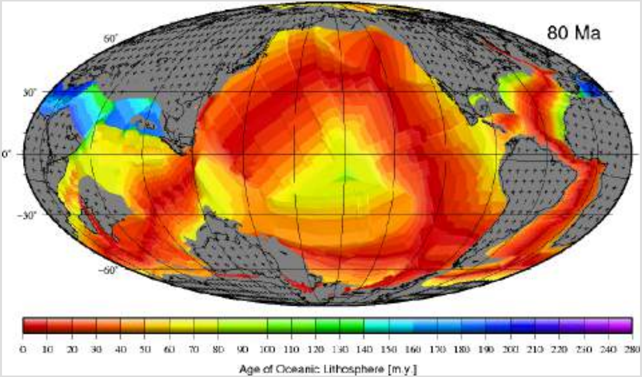

Record of past (late Mesozoic/Cenozoic) plate motion:

horizontal motion of Earth's surface is reconstructed for past $\approx$ 200 million years

provides boundary condition for velocity

one effectively exploits Serrin's theorem

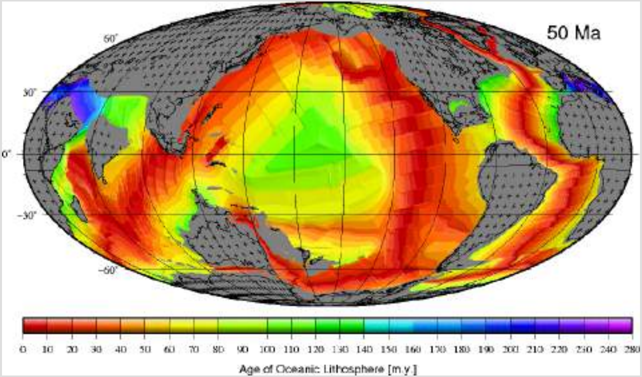

Record of past (late Mesozoic/Cenozoic) plate motion:

horizontal motion of Earth's surface is reconstructed for past $\approx$ 200 million years

provides boundary condition for velocity

one effectively exploits Serrin's theorem

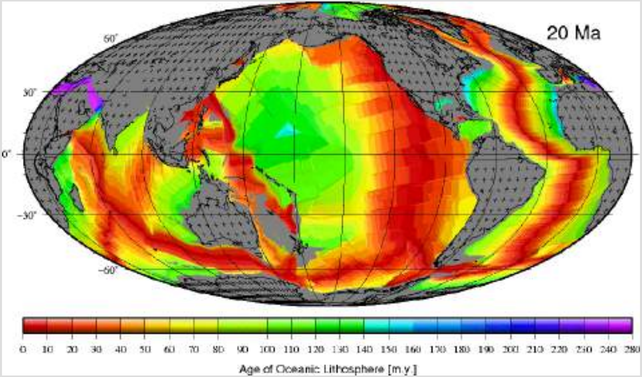

Record of past (late Mesozoic/Cenozoic) plate motion:

horizontal motion of Earth's surface is reconstructed for past $\approx$ 200 million years

provides boundary condition for velocity

one effectively exploits Serrin's theorem

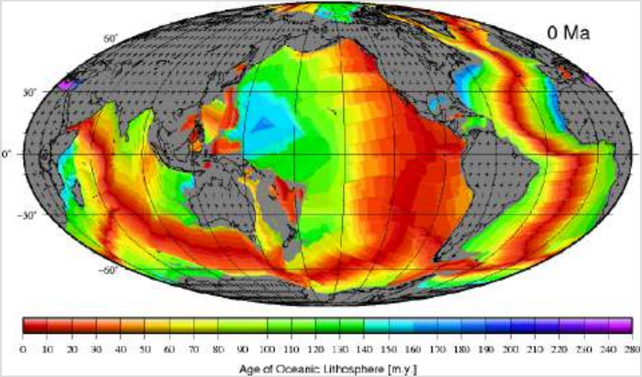

compressibility effects

(These should be included, if one wants to apply geodynamic adjoint models to seismically inferred Earth structure.)

Twin Experiments (compressible)

Evolve Reference Twin (right column) from *initial* to *final* state.

Time period corresponding to 50 Myrs ($\approx 1/2$ overturn).

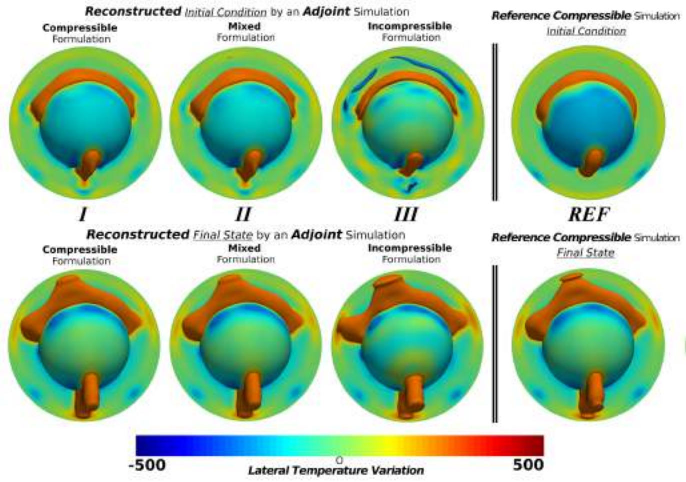

Initial and final state reconstructions for consistent (left), mixed (middle) and inconsistent (right) model (red=hot, blue=cold). Reference Twin (right most figure)
(from **Ghelichkhan & Bunge, 2016**)

Twin Experiments (compressible)

Evolve Reference Twin (right column) from *initial* to *final* state.

Time period corresponding to 50 Myrs ($\approx 1/2$ overturn).

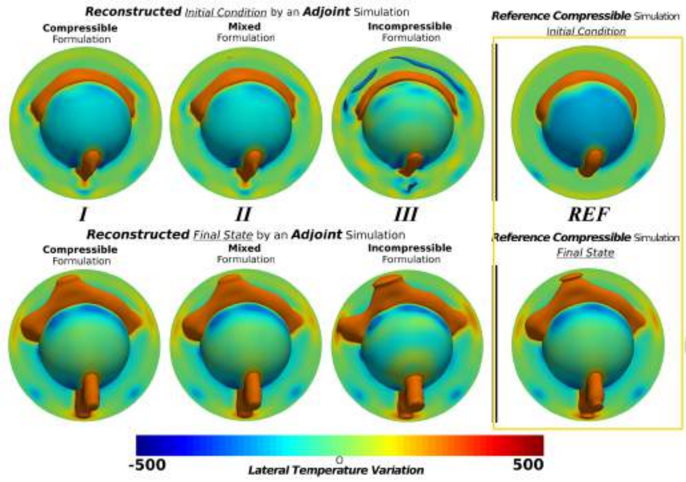

Initial and final state reconstructions for consistent (left), mixed (middle) and inconsistent (right) model (red=hot, blue=cold). Reference Twin (right most figure)
(from **Ghelichkhan & Bunge, 2016**)

Twin Experiments (compressible)

Evolve Reference Twin (right column) from *initial* to *final* state.

Time period corresponding to 50 Myrs ($\approx 1/2$ overturn).

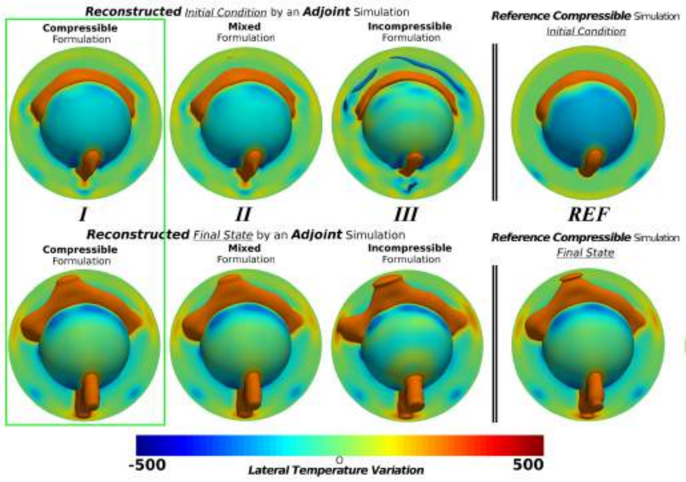

Initial and final state reconstructions for consistent (left), mixed (middle) and inconsistent (right) model (red=hot, blue=cold). Reference Twin (right most figure)
(from **Ghelichkhan & Bunge, 2016**)

Twin Experiments (compressible)

Evolve Reference Twin (right column) from *initial* to *final* state.

Time period corresponding to 50 Myrs ($\approx 1/2$ overturn).

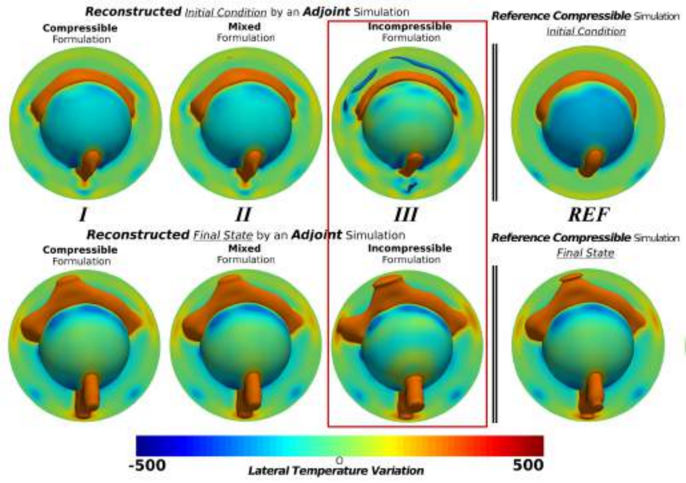

Initial and final state reconstructions for consistent (left), mixed (middle) and inconsistent (right) model (red=hot, blue=cold). Reference Twin (right most figure)
(from **Ghelichkhan & Bunge, 2016**)

Twin Experiments

Final State
RMS error as a function of adjoint iteration
Note: There is convergence, i.e. the cost function is reduced, for all cases.

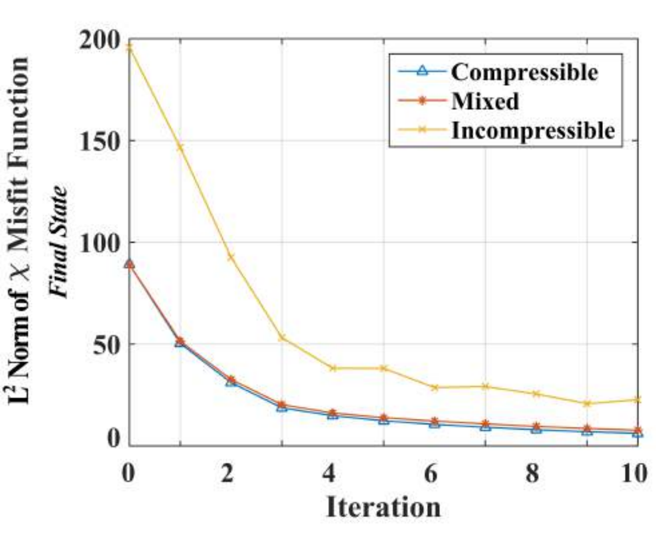

(from **Ghelichkhan & Bunge, 2016**)

Twin Experiments

Initial State
RMS error as a function of adjoint iteration
Note: Inconsistent formulations lead to convergence error in the initial state, as expected.

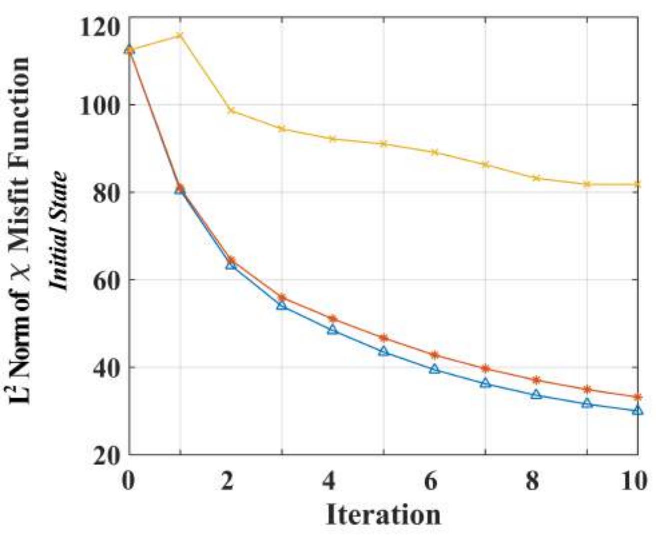

(from **Ghelichkhan & Bunge, 2016**)

Twin Experiments

Initial State

RMS error as a function of adjoint iteration

Note: Inconsistent formulations lead to convergence error in the initial state, as expected.

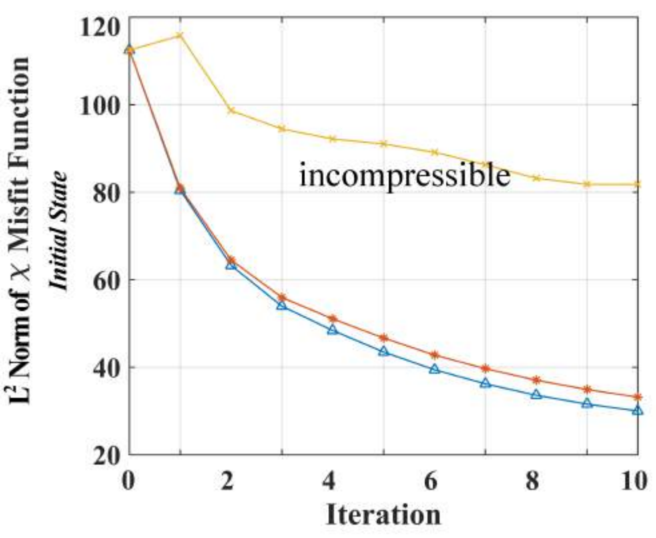

(from **Ghelichkhan & Bunge, 2016**)

Twin Experiments

Final State error.

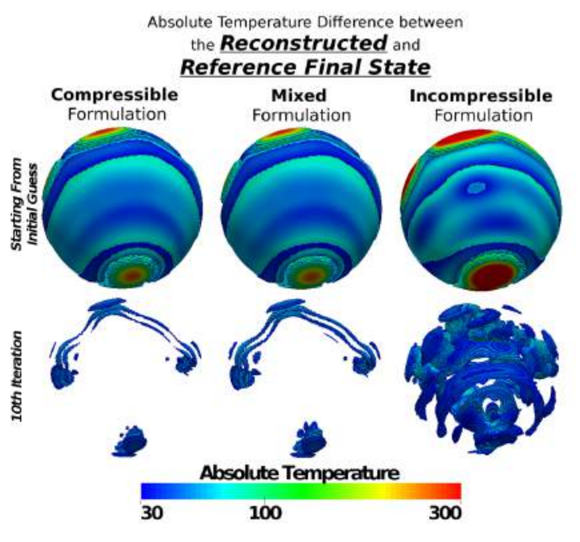

(from **Ghelichkhan & Bunge, 2016**)

Twin Experiments

Final State error.

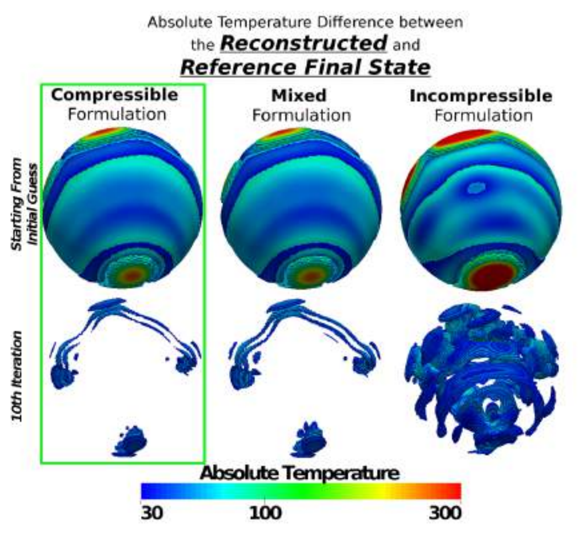

(from **Ghelichkhan & Bunge, 2016**)

Twin Experiments

Final State error.

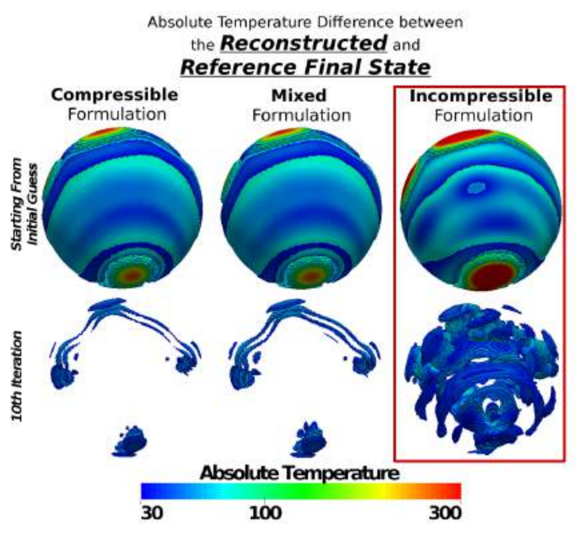

(from **Ghelichkhan & Bunge, 2016**)

Application of simple Geodynamic Earth models (GEMS) to seismic structure

(Uniqueness, and effect of model initialisation)

Heterogeneity (Geodynamic Models, Mineral Physics)

- Schuberth et al., 2009a,b, Davies et al., 2012
- Schaber et al., 2009
- Goal:
  - compare geodynamic with seismic models by going through the convection process and mapping geodynamic to elastic variation

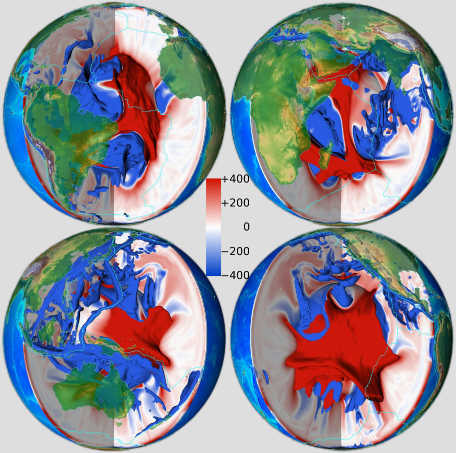

Simple Geodynamic Earth Models

Final State
3 viscosity layers
Isochemical
80 million grid points

initialized from **present-day** structure for unknown heterogeneity *40 million years* ago

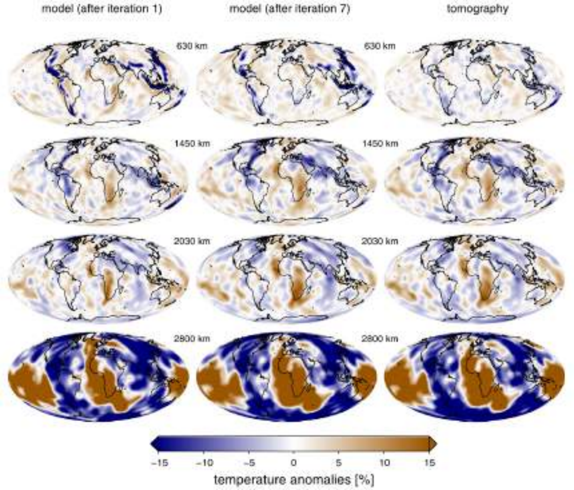

(from **Horbach et al., 2014**)

Simple Geodynamic Earth Models

Initial State Corrections
shown after 1 (left), 2 (middle) and 7 (right) iterations

only small corrections are needed after 7 iterations (right most column)

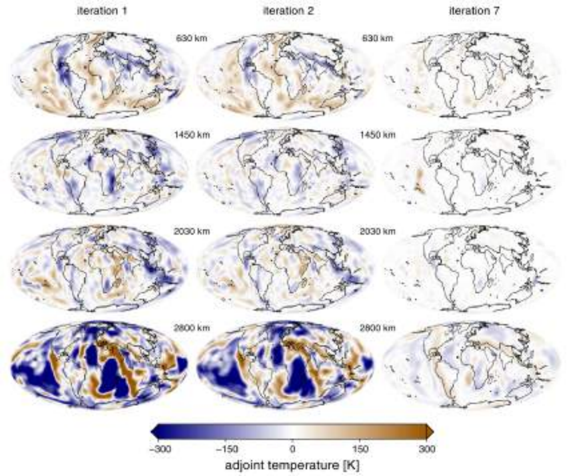

(from **Horbach et al., 2014**)

Simple Geodynamic Earth Models

Optimal **Initial State**
40 million years ago
3 viscosity layers
Isochemical
80 million grid points

initialized from
present-day structure
for unknown
heterogeneity *40 million years* ago

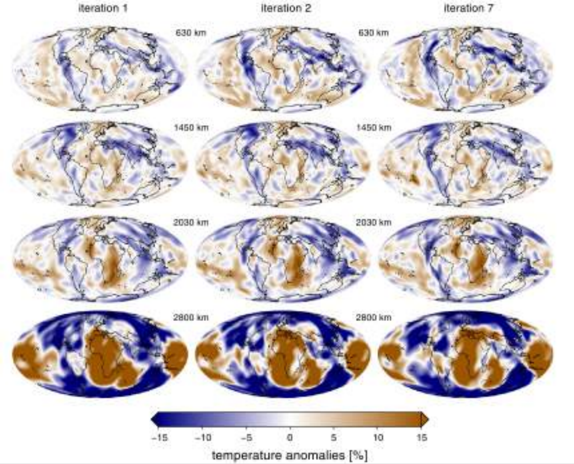

(from **Horbach et al., 2014**)

Simple Geodynamic Earth Models

Sensitivity to First Guess choice

present-day (a), rotated (b), blank (c), backward advection (d)

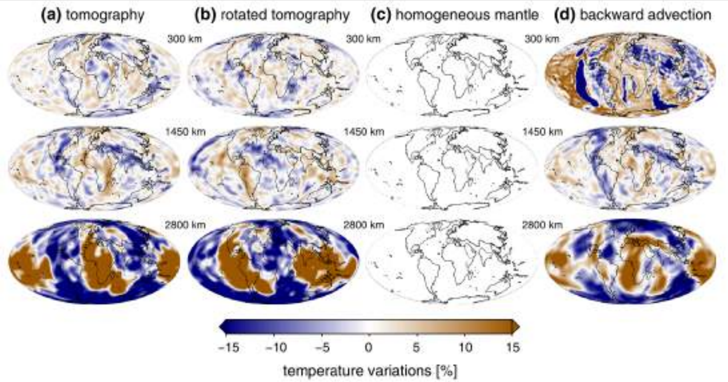

(from **Horbach et al., 2014**)

Simple Geodynamic Earth Models

Optimal Initial State computed from **four** different First Guesses present-day (a), rotated (b), blank (c), backward advection (d)

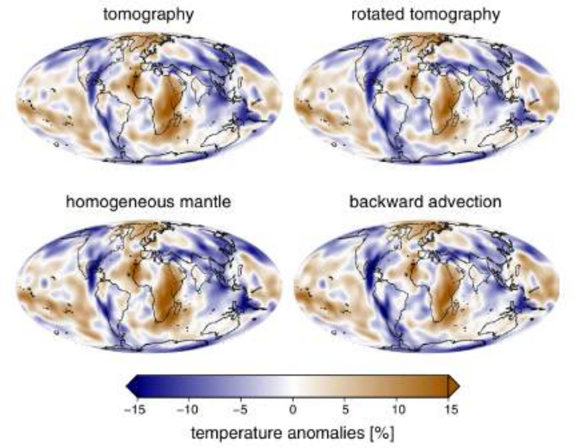

(from **Horbach et al., 2014**)

Application (different guesses for initial state)

Residual at final state vs. Iteration for four ' initial guess' models: a) tomo b) rotated tomo c) blank mantle d) backw. advection.

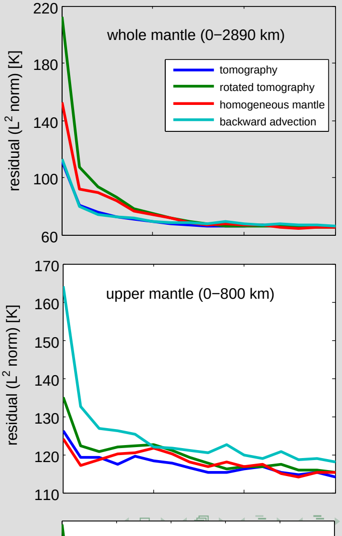

Backward advection (cyan curve on the right) is a poor initialisation for upper mantle structure

Retrodictions

Global High Resolution ($\approx$ 670 million grid points) Geodynamic Earth Models

(sensitivity to tomographic input model and viscosity profile)

Model Overview

- ($\approx$ 670 million grid points), grid point distance $\approx 10km$
- per adjoint iteration $\approx$ 1 million Core Hours
- six adjoint iterations per model
- four different models with Earthlike convective vigor
- pyrolite composition assumed for the sake of simplicity
- sensitivity to tomographic input structure and lower mantle viscosity

Tomographic input model

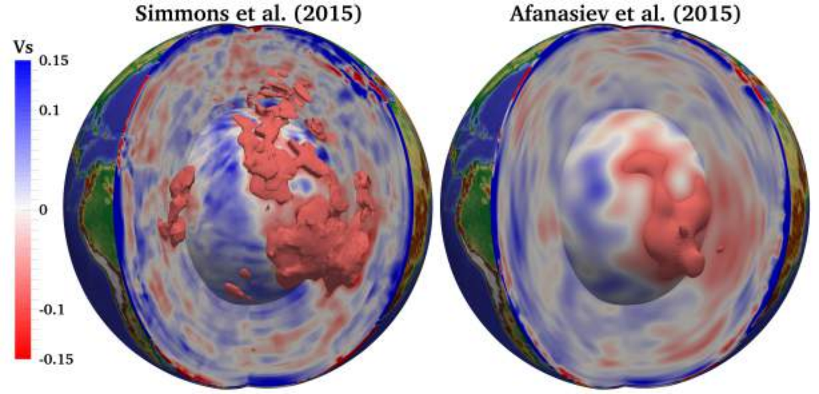

(from **Colli et al., 2017**)

Viscosity profiles and dynamic topography kernels

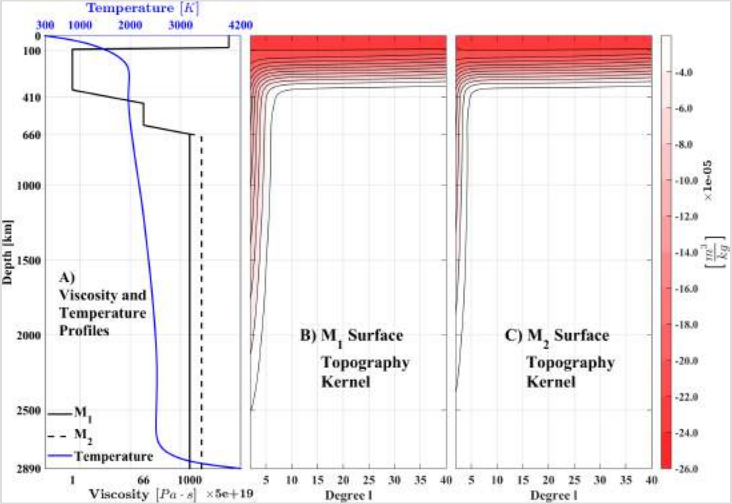

(from **Colli et al., 2017**)

Conversion from Elastic to Geodynamic heterogeneity

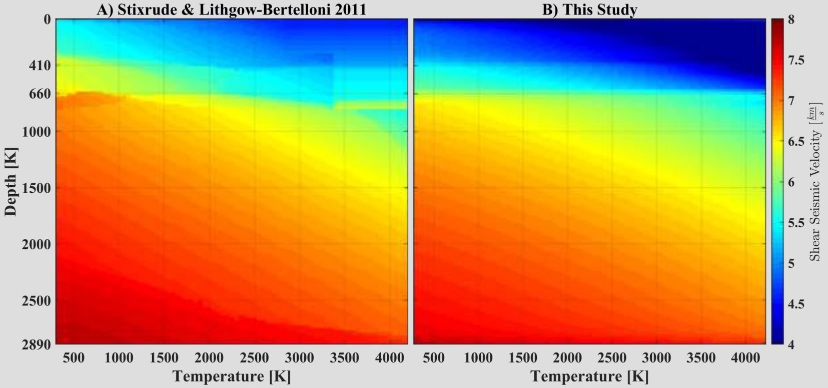

(from **Colli et al., 2017**)

Misfit Reduction

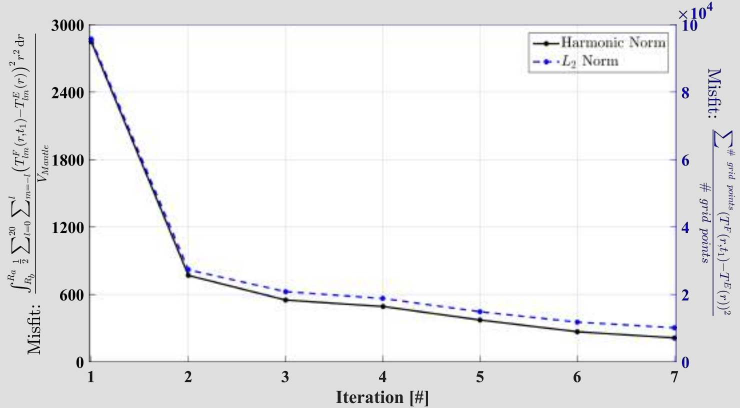

(from **Colli et al., 2017**)

Hemispheric Retrodictions (Atlantic Realm)

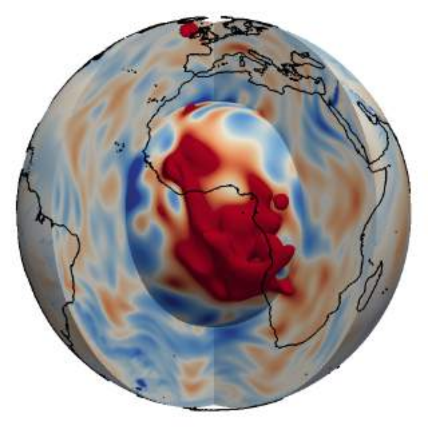

Thermal Field for AM2 at Final State (today)

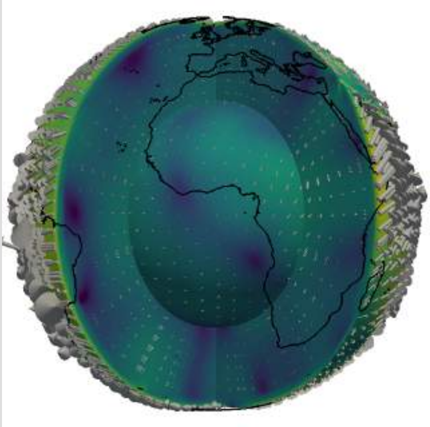

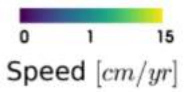

Velocity Field for AM2 at Final State (today)

Histograms

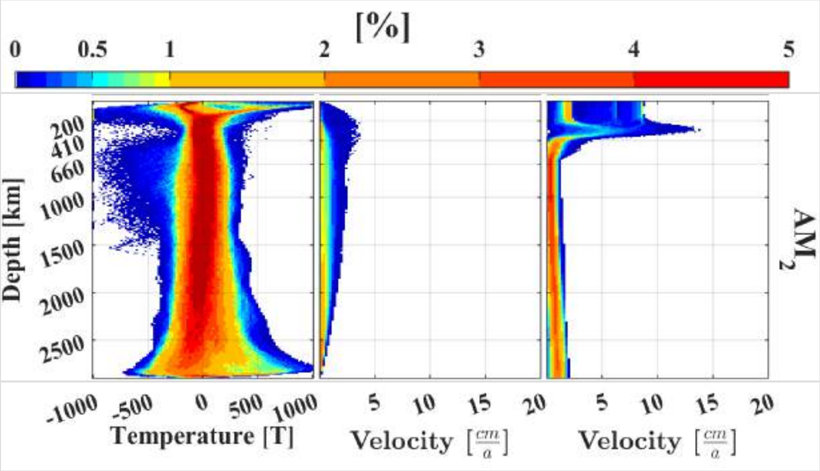

(from **Colli et al., 2017**)

Hemispheric Retrodictions (Atlantic Realm)

Model AM2

40 Ma

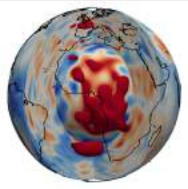

Whole Mantle Model Thermal Field

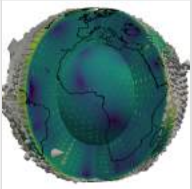

Whole Mantle Model Flow Velocities

Upper Mantle Temperature

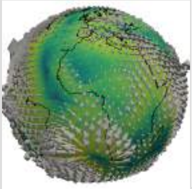

Upper Mantle Flow Velocities

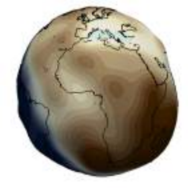

Dynamic Topography (lmax 20)

Hemispheric Retrodictions (Atlantic Realm)

Model AM2

35 Ma

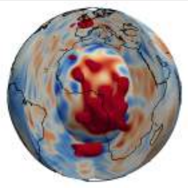

Whole Mantle Model Thermal Field

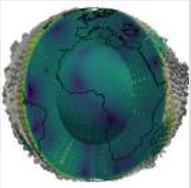

Whole Mantle Model Flow Velocities

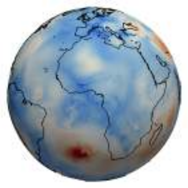

Upper Mantle Temperature

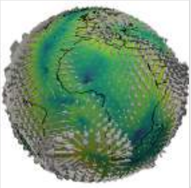

Upper Mantle Flow Velocities

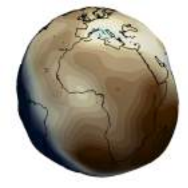

Dynamic Topography (lmax 20)

Hemispheric Retrodictions (Atlantic Realm)

Model AM2

30 Ma

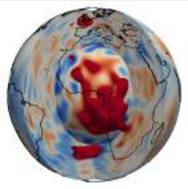

Whole Mantle Model Thermal Field

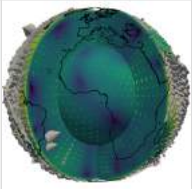

Whole Mantle Model Flow Velocities

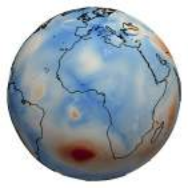

Upper Mantle Temperature

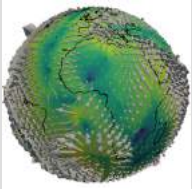

Upper Mantle Flow Velocities

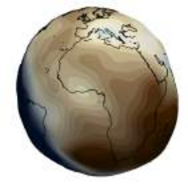

Dynamic Topography (lmax 20)

Hemispheric Retrodictions (Atlantic Realm)

Model AM2

25 Ma

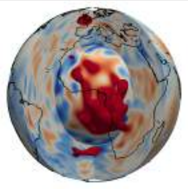

Whole Mantle Model Thermal Field

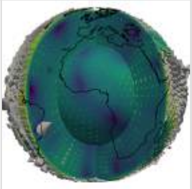

Whole Mantle Model Flow Velocities

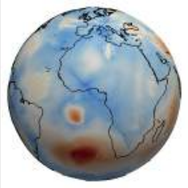

Upper Mantle Temperature

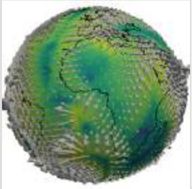

Upper Mantle Flow Velocities

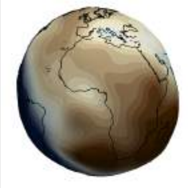

Dynamic Topography (lmax 20)

Hemispheric Retrodictions (Atlantic Realm)

Model AM2

20 Ma

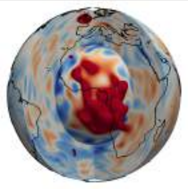

Whole Mantle Model Thermal Field

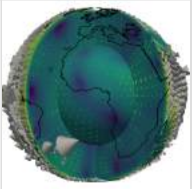

Whole Mantle Model Flow Velocities

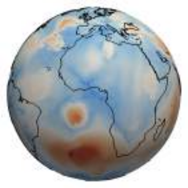

Upper Mantle Temperature

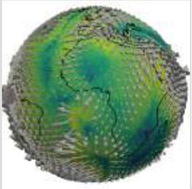

Upper Mantle Flow Velocities

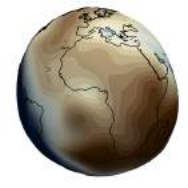

Dynamic Topography (lmax 20)

Hemispheric Retrodictions (Atlantic Realm)

Model AM2

15 Ma

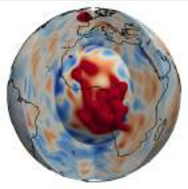

Whole Mantle Model Thermal Field

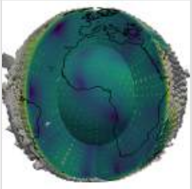

Whole Mantle Model Flow Velocities

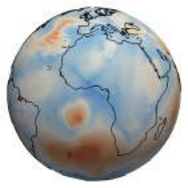

Upper Mantle Temperature

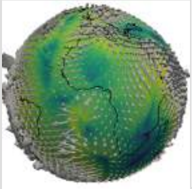

Upper Mantle Flow Velocities

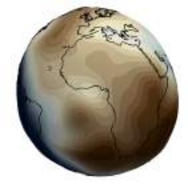

Dynamic Topography (lmax 20)

Hemispheric Retrodictions (Atlantic Realm)

Model AM2

10 Ma

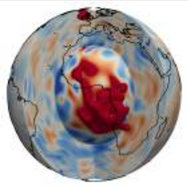

Whole Mantle Model Thermal Field

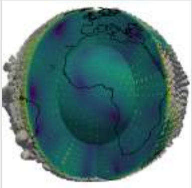

Whole Mantle Model Flow Velocities

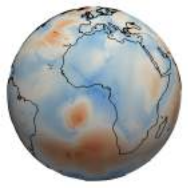

Upper Mantle Temperature

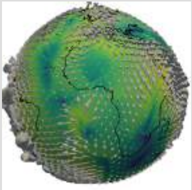

Upper Mantle Flow Velocities

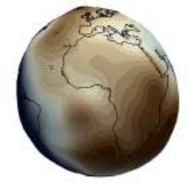

Dynamic Topography (lmax 20)

Hemispheric Retrodictions (Atlantic Realm)

Model AM2

5 Ma

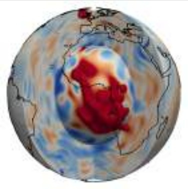

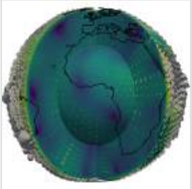

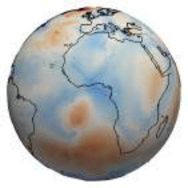

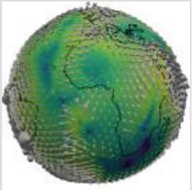

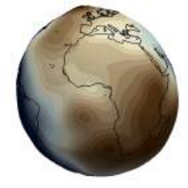

Whole Mantle Model Thermal Field	**Whole Mantle Model Flow Velocities**	**Upper Mantle Temperature**	**Upper Mantle Flow Velocities**	**Dynamic Topography (lmax 20)**

Hemispheric Retrodictions (Atlantic Realm)

Model AM2

today

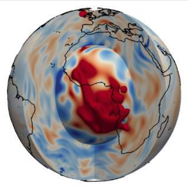

Whole Mantle Model

Thermal Field

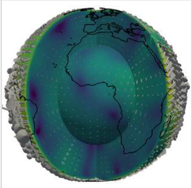

Whole Mantle Model

Flow Velocities

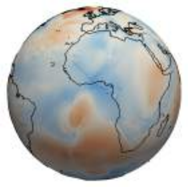

Upper Mantle

Temperature

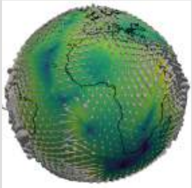

Upper Mantle Flow

Velocities

Dynamic Topography

(lmax 20)

Regional Retrodictions (North Atlantic/W.Europe)

40 Ma

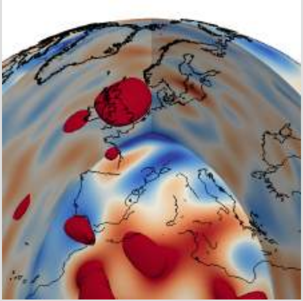

Thermal Field

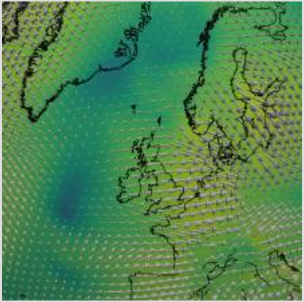

Upper Mantle Velocity

Dynamic Topography (lmax 40)

Regional Retrodictions (North Atlantic/W.Europe)

35 Ma

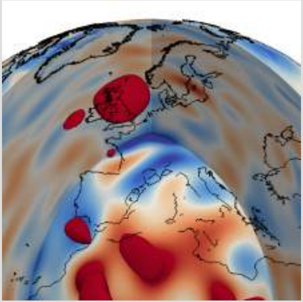

Thermal Field

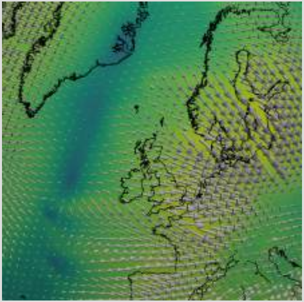

Upper Mantle Velocity

Dynamic Topography (lmax 40)

Regional Retrodictions (North Atlantic/W.Europe)

30 Ma

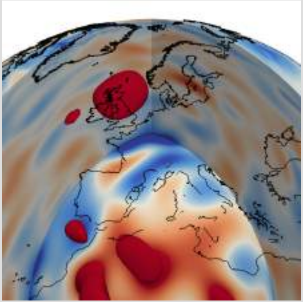

Thermal Field

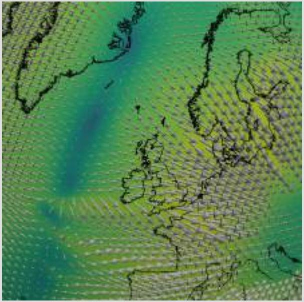

Upper Mantle Velocity

Dynamic Topography (lmax 40)

Regional Retrodictions (North Atlantic/W.Europe)

25 Ma

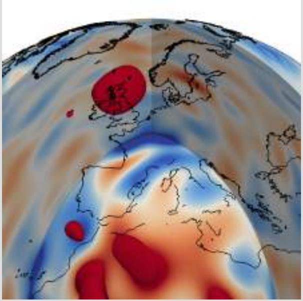

Thermal Field

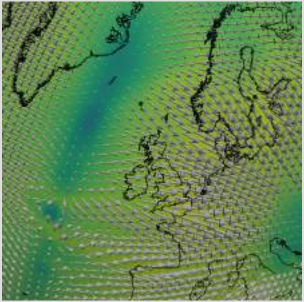

Upper Mantle Velocity

Dynamic Topography (lmax 40)

Regional Retrodictions (North Atlantic/W.Europe)

20 Ma

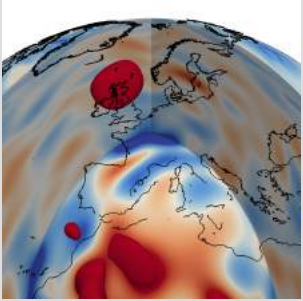

Thermal Field

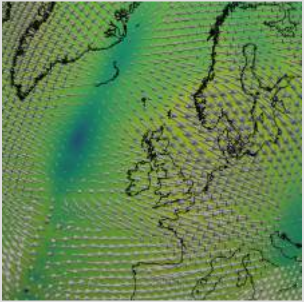

Upper Mantle Velocity

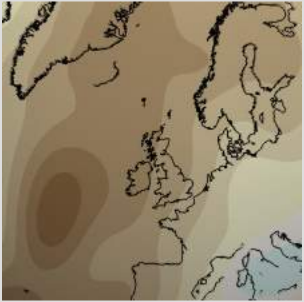

Dynamic Topography (lmax 40)

Regional Retrodictions (North Atlantic/W.Europe)

15 Ma

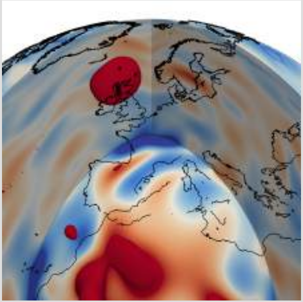

Thermal Field

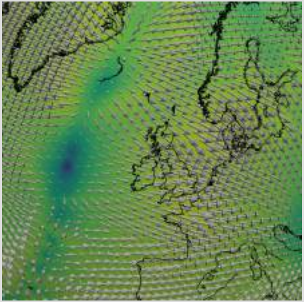

Upper Mantle Velocity

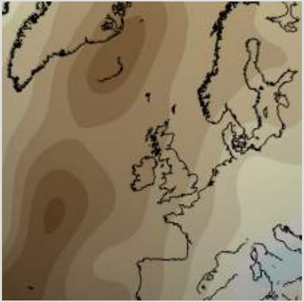

Dynamic Topography (lmax 40)

Regional Retrodictions (North Atlantic/W.Europe)

10 Ma

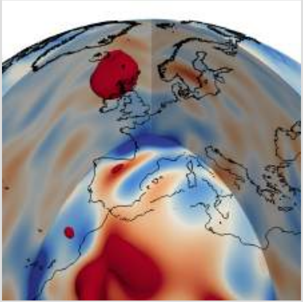

Thermal Field

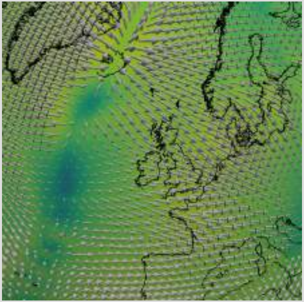

Upper Mantle Velocity

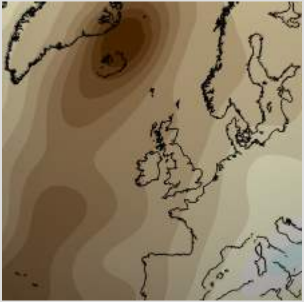

Dynamic Topography (lmax 40)

Regional Retrodictions (North Atlantic/W.Europe)

5 Ma

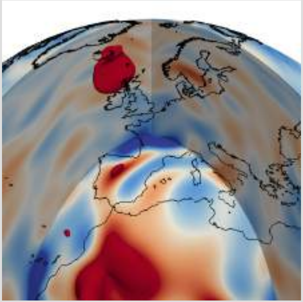

Thermal Field

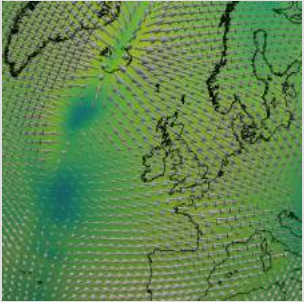

Upper Mantle Velocity

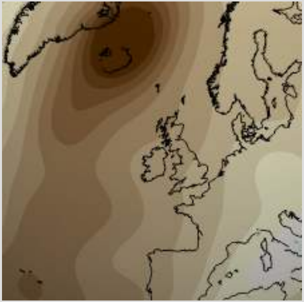

Dynamic Topography (lmax 40)

Regional Retrodictions (North Atlantic/W.Europe)

today

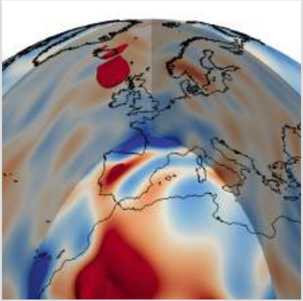

Thermal Field

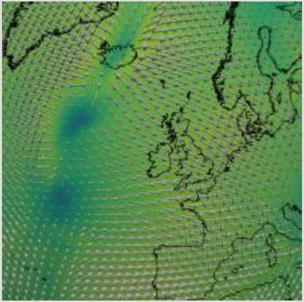

Upper Mantle Velocity

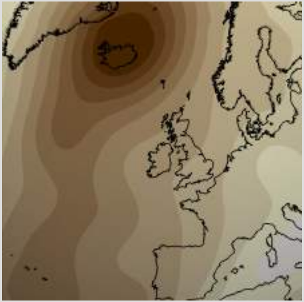

Dynamic Topography (lmax 40)

Geology

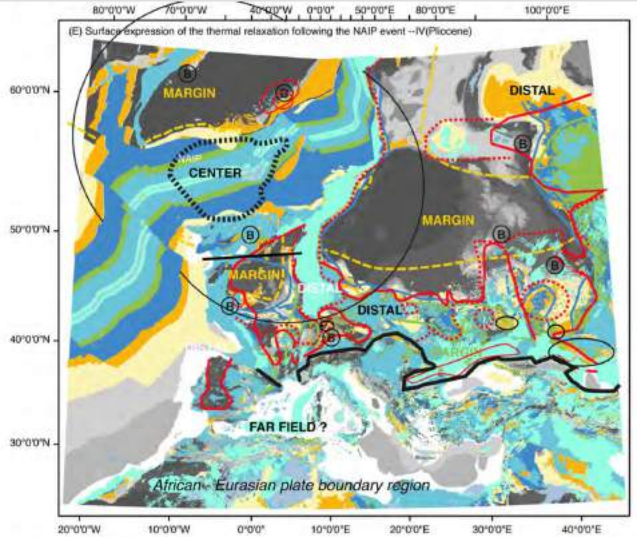

(from **Friedrich et al., 2017**)

Paris

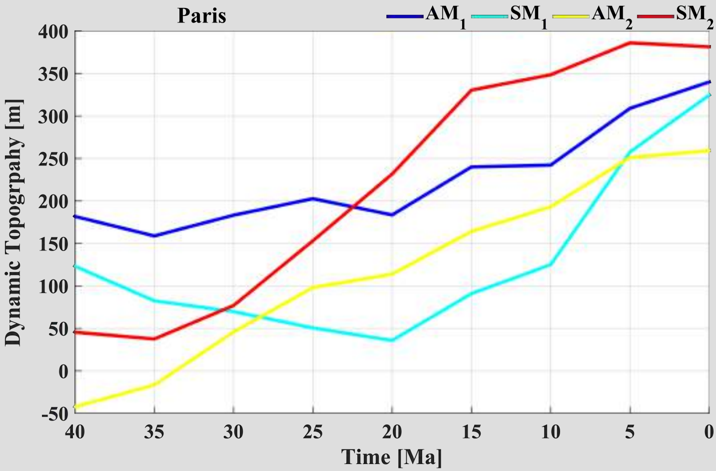

(from **Colli et al., 2017**)

Computational aspects

- $10^9 - 10^{10}$ free parameters (resolution dependent)
- iterative conjugate gradient scheme
- ≈ 10 iterations needed to reach convergence
- 1 forward and 1 adjoint simulation per iteration
- need to store u and T at each time-step in the forward simulation
- forward and adjoint equations are similar
  $\rightarrow$ same numerical code can be used
- **This is expensive.**

Conclusion

Growing model complexity makes it attractive to *test* geodynamic simulations by retrodictions

Uniqueness properties make plate motions the *input* rather than the output of a retrodiction

Compressible adjoint equations allow us to apply retrodictions to seismically derived mantle structure

Retrodictions open exiting possibilities for collaborative work *across* the Earth Sciences